



Syntheses, luminescences and Hirshfeld surfaces analyses of structurally characterized homo-trinuclear Zn^{II} and hetero-pentanuclear Zn^{II}-Ln^{III} (Ln = Eu, Nd) bis(salamo)-like complexes

Qing Zhao, Xiao-Xin An, Ling-Zhi Liu, Wen-Kui Dong*

School of Chemical and Biological Engineering, Lanzhou Jiaotong University, Lanzhou, Gansu 730070, PR China



ARTICLE INFO

Keywords:

Bis(salamo) ligand
Zn^{II}-Ln^{III} complex
Crystal structure
Hirshfeld surface analysis
Luminescence

ABSTRACT

Homo-trinuclear [Zn₃(L)(μ₂-OAc)₂(H₂O)]·CH₂Cl₂ (**1**) and hetero-pentanuclear [Zn₄(L)₂Eu(NO₃)₃(H₂O)] (**2**) and [Zn₄(L)₂Nd(NO₃)₃(H₂O)]·CH₃CH₂OH (**3**) complexes containing a coumarin-skeleton bis(salamo) ligand H₄L, were successfully prepared and characterized via the means of elemental analyses, single crystal X-ray crystallography, FT-IR, UV-Vis absorption spectroscopy and Hirshfeld surfaces analyses. Complex **1** is a 1:3 ((L)⁴⁻:Zn^{II}) structure, and complexes **2** and **3** are 2:4:1 ((L)⁴⁻:Zn^{II}:Ln^{III}) structure. All Zn^{II} atoms in complexes **1–3** occupied the N₂O₂ sites are five-coordinated with geometries of slightly distorted tetragonal pyramid and trigonal bipyramid. Rare earth metal (Eu^{III} and Nd^{III}) atoms are both coordinated with phenolic oxygen atoms, and eight-coordinated with the square antiprism geometries in complexes **2** and **3**. Water molecules as coordinating solvents participate in the coordination. Supra-molecular structures are built by C–H···π and hydrogen bonding interactions in complexes **1–3**. Moreover, Hirshfeld surfaces analyses of complexes **1–3** were also analysed in detail. Most important of all, luminescences of complexes **1–3** were discussed.

1. Introduction

Recently, the extensive research on the metal complexes has been received increase attention in the fields of coordination chemistry and organometallic chemistry. Salen-like ligands having O, N-donor sites are apt to coordinate to transition metal ions [1,2]. Consequently, salen-like complexes also have been actively studied because of not only their interesting crystal structures but also their widespread applications, such as catalysts for organic reactions [3–5], electrochemical conducts [6,7], magnetic materials [8–13], luminescences [14–17], ions recognitions [18–22], supra-molecular buildings [23,24], non-linear optical materials [25] and biological systems [26–28].

Noticeably, salamo-like ligands [29–33], as a salen-like derivative, have been developed by Nabeshima's group [34,35], mainly using to synthesize transition and rare metal complexes. Compared with transition metal ions, lanthanide ions possess the characteristics of high coordination numbers and electronic structure. Accordingly, the structures of lanthanide complexes are interesting [36–38]. A great quantity of studies on the lanthanide complexes arise from their extensive applications such as biomedical and optical technologies. Salamo-like zinc(II) complexes have been widely researched due to their interesting photophysical properties [39–41]. Many efforts have

been devoted to the preparations of Zn^{II}-Ln^{III} complexes because of their potential applications in magnetic [42–44] and supra-molecular architectures [45–49]. Coumarin, as an important intermediate product and raw materials of organic chemicals, has been widely used in medicine, agriculture, photosensitive materials and other fields. It is noteworthy that coumarin and its derivatives have good characteristics of luminescences [33,50,51] and can be used as a good luminescent material.

Based on previous researches, in this paper, we designed a new containing coumarin-skeleton bis(salamo)-like ligand H₄L, and obtained three homo-trinuclear Zn^{II} (**1**) and hetero-pentanuclear Zn^{II}-Ln^{III} (Ln = Eu (**2**) and Nd(**3**)) complexes by the metalation of H₄L. To our best knowledge, these hetero-pentanuclear 2:5 ((L)⁴⁻:Mⁿ⁺) bis(salamo)-like complexes has rarely reported [6]. Most important of all, the Hirshfeld surfaces analyses and spectroscopic properties of complexes **1–3** were investigated in detail.

2. Experimental

2.1. Materials and methods

1,2-Dimethoxybenzene, *n*-butyllithium, TMEDA, boron tribromide

* Corresponding author.

E-mail address: dongwk@126.com (W.-K. Dong).

<https://doi.org/10.1016/j.ica.2019.02.040>

Received 3 February 2019; Received in revised form 24 February 2019; Accepted 26 February 2019

Available online 27 February 2019

0020-1693/ © 2019 Elsevier B.V. All rights reserved.

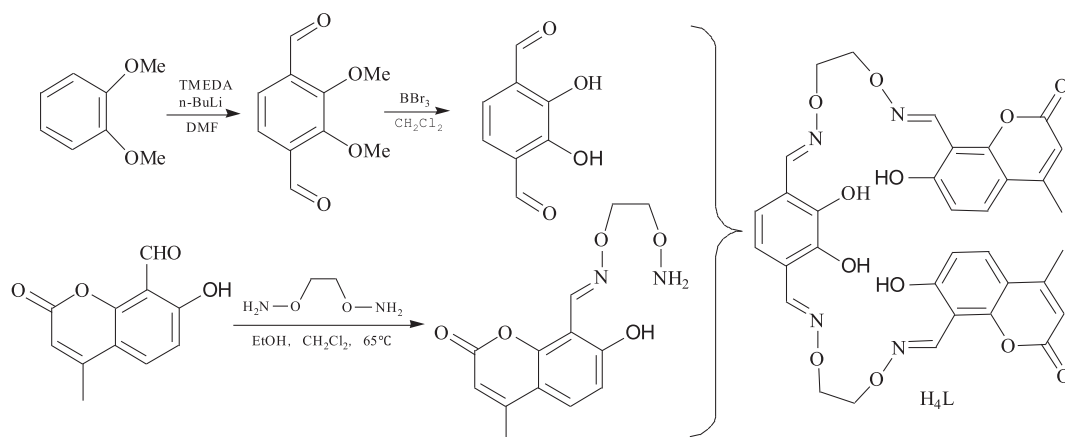
Scheme 1. Synthetic route to H₄L.

Table 1
Crystal and refinement parameter data for complexes 1–3.

Complex	1	2	3
Empirical formula	C ₃₉ H ₃₆ Cl ₂ Zn ₃ N ₄ O ₁₇	C ₆₈ H ₅₄ Zn ₄ EuN ₁₁ O ₃₄	C ₇₀ H ₆₀ Zn ₄ NdN ₁₁ O ₃₅
Formula weight	1099.73	1982.66	2021.01
T (K)	173.00(10)	294.21(11)	173.00(10)
Wavelength (Å)	1.54184	0.71073	0.71073
Crystal system	triclinic	monoclinic	monoclinic
Space group	<i>P</i> -1	<i>P</i> 2/ <i>n</i>	<i>P</i> 2 ₁ / <i>n</i>
<i>a</i> (Å)	9.7720(5)	11.8043(5)	12.0044(3)
<i>b</i> (Å)	15.1890(7)	18.7183(7)	33.8551(8)
<i>c</i> (Å)	15.7665(5)	21.9339(9)	22.8025(5)
α (°)	66.402(4)	90	90
β (°)	79.564(4)	91.662(4)	97.531(2)
γ (°)	79.188(4)	90	90
<i>V</i> (Å ³)	2091.73(17)	4844.4(3)	9187.3(4)
<i>Z</i>	2	2	4
<i>D</i> _{calc} (g·cm ⁻³)	1.746	1.359	1.461
Absorption coefficient (mm ⁻¹)	3.895	1.692	1.669
θ range for data collection (°)	3.501–66.599	3.370–26.022	3.424–26.022
<i>F</i> (0 0 0)	1116.0	1988.0	4068.0
<i>h</i> / <i>k</i> / <i>l</i> (minimum, maximum)	–11, 9/–18, 18/–18, 16	–14, 14/–20, 23/–16, 27	–14, 13/–41, 39/–17, 28
Crystal size (mm)	0.12 × 0.14 × 0.15	0.14 × 0.16 × 0.18	0.14 × 0.15 × 0.21
Reflections collected <i>R</i> _{int}	13757/7179	19845/9533	35,539/18,052
	0.0214	0.0394	0.0386
Independent reflection	6494	6621	12,757
Completeness to θ (%)	96.92	99.73	99.71
Data/restraints/parameters	7179/27/616	9533/63/549	18052/126/1142
Final <i>R</i> indices [<i>I</i> > 2 σ (<i>I</i>)]	<i>R</i> ₁ = 0.0542, <i>wR</i> ₂ = 0.1452	<i>R</i> ₁ = 0.0472, <i>wR</i> ₂ = 0.1046	<i>R</i> ₁ = 0.0533, <i>wR</i> ₂ = 0.1015
<i>R</i> indices (all data)	<i>R</i> ₁ = 0.0589, <i>wR</i> ₂ = 0.1500	<i>R</i> ₁ = 0.0743, <i>wR</i> ₂ = 0.1192	<i>R</i> ₁ = 0.0824, <i>wR</i> ₂ = 0.1161
Goodness-of-fit for (<i>F</i> ²)	1.038	1.031	1.032
Largest difference peak and hole (e Å ⁻³)	1.705, –1.847	0.698, –0.570	0.830, –0.508

$$^a R_1 = \frac{\sum ||F_o| - |F_c||}{\sum |F_o|}$$

$$^b wR_2 = \frac{[\sum w(F_o^2 - F_c^2)^2 / \sum w(F_o^2)^2]^{1/2}}{w}, w = [\sigma^2(F_o^2) + (0.0784P)^2 + 1.3233P]^{-1}, \text{ where } P = (F_o^2 + 2F_c^2)/3.$$

$$^c \text{GOF} = \frac{[\sum w(F_o^2 - F_c^2)^2 / n_{\text{obs}} - n_{\text{param}}]^{1/2}}{}$$

and 7-hydroxyl-4-methylcoumarin (98%) were purchased from Alfa Aesar and used directly without purification. All other commercially available solvents and chemicals were analytical reagent and bought from Tianjin Chemical Reagent Factory. Elemental analyses (C, H and N) were performed on a GmbH VarioEL V3.00 automatic elemental analysis instrument. Elemental analyses for metals were carried out on an IRIS ER/S-WP-1 ICP atomic emission spectrometer. Fourier transform Infrared spectra were conducted by using CsI (100–500 cm⁻¹) and KBr (500–4000 cm⁻¹) pellets on a VERTEX70 FT-IR spectrophotometer. UV–Vis absorption spectra were collected on a Shimadzu UV-3900 spectrophotometer. Luminescent spectra were obtained on F-7000 spectrophotometer. Melting points were collected on a microscopic melting point apparatus made by Beijing Taike Instrument

Limited Company. Single crystal X-ray structure determinations were determined by a SuperNova Dual, Cu at zero, Eos four-circle diffractometer. Hirshfeld surface analyses and two-dimensional fingerprint plots of complexes 1–3 were calculated using Crystal Explorer program.

2.2. Synthesis of bis(salomo) ligand H₄L

1,2-Bis(aminooxy)ethane and 8-formyl-7-hydroxy-4-methylcoumarin were synthesized in accordance with the previously literatures [52,53]. Major synthetic route of H₄L is presented in Scheme 1.

8-Formyl-7-hydroxy-4-methylcoumarin (408.3 mg, 2.0 mmol) dissolved in the methanol solution (30 mL) was slowly added to a colorless

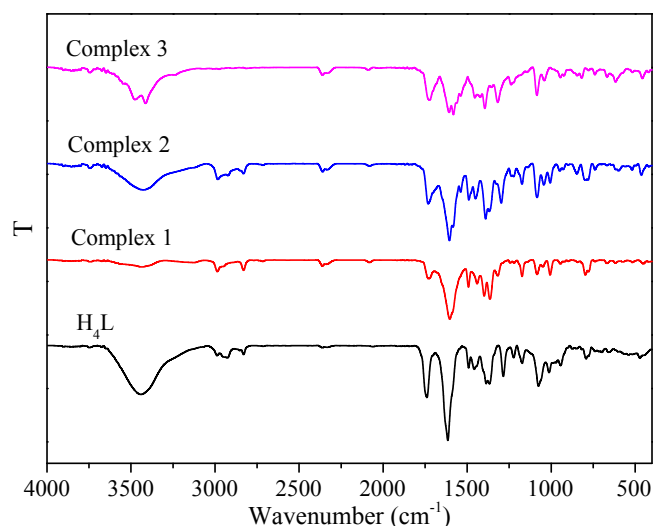


Fig. 1. FT-IR spectra of H_4L and its complexes 1–3.

methanol solution (30 mL) of 1,2-bis(aminoxy)ethane (184.2 mg, 2.0 mmol) and heated to reflux at 80 °C more than 4 h. Subsequently, the mixture solution was concentrated via vacuum distillation. The mixture was separated by column chromatography using ethyl acetate: chloroform = 1:5 and obtained 417.4 mg white intermediate product 2-[O-(1-ethoxyamide)]oxime-4-methylcoumarinphenol.

A yellow ethanol solution (10 mL) of 2, 3-dihydroxybenzene-1,4-dicarbaldehyde (83.1 mg, 0.5 mmol) was slowly added to a dichloromethane solution (10 mL) of above-mentioned 2-[O-(1-ethoxyamide)]oxime-4-methylcoumarinphenol (278.3 mg, 1.0 mmol). The mixture solution was heated and refluxed at 65 °C about 3 h before being allowed to cool to room temperature. Subsequently, the solution was filtered and washed with ethanol/hexane (1:4). Finally, the yellow solid of H_4L was collected. Yield, 42.5%. M.p. 181–182 °C. *Anal. Calc.* for $C_{34}H_{30}N_4O_{12}$: C, 59.47; H 4.40; N, 8.16. Found: C, 59.69; H, 4.64; N, 8.01%. IR (KBr; cm^{-1}): 1617 [$\nu(C=N)$], 1279 [$\nu(Ar-O)$], 1751 [$\nu(C=O)$], 3444 [$\nu(O-H)$]. UV-Vis [in chloroform/ethanol (1:1)], λ_{max} (nm) [2.5×10^{-5} M]: 285, 302, 316, 344.

2.3. Synthesis of homotrimeric complex 1

$Zn(OAc)_2$ (6.59 mg, 0.03 mmol) dissolved in ethanol solution (2 mL) of was added to dichloromethane solution (3 mL) of H_4L (6.87 mg, 0.01 mmol). The mixture solution was stirred at room temperature for 25 min, and the color of the solution turned yellow. Then, the mixture was filtered and stood at room temperature approximately three weeks. Several clear light colourless crystals were collected. Yield, 33.7%. *Anal. Calc.* for $[Zn_3(L)(\mu_2-OAc)_2(H_2O)_2] \cdot CH_2Cl_2$ ($C_{39}H_{36}Cl_2Zn_3N_4O_{17}$): C 42.59; H, 3.30; N, 5.09; Zn, 17.84. Found: C, 42.72; H, 3.48; N, 4.88; Zn, 17.61%. IR (KBr; cm^{-1}): 1604 [$\nu(C=N)$], 1181 [$\nu(Ar-O)$], 1731 [$\nu(C=O)$]. UV-Vis [in ethanol], λ_{max} (nm) [1.0×10^{-3} M]: 292, 312, 318, 356.

2.4. Synthesis of heteropentanuclear complexes 2 and 3

$Zn(OAc)_2$ (8.78 mg, 0.04 mmol) and $Ln(NO_3)_3$ ($Ln = Eu, Nd$) (4.46 mg, 0.01 mmol) was dissolved in ethanol solution (2 mL), respectively. The above solutions (4 mL) were added to the chloroform solution (2.0 mL) of H_4L (13.74 mg, 0.02 mmol). Subsequently, the color of the mixed solution became yellow and was stirred for 40 min. Then, the solution was filtered and stood undisturbed for about one month at room temperature. Clear block-like yellow crystals for X-ray crystallographic analysis were gained.

For $[Zn_4Eu]$ complex 2, block-like transparent dark yellow crystals.

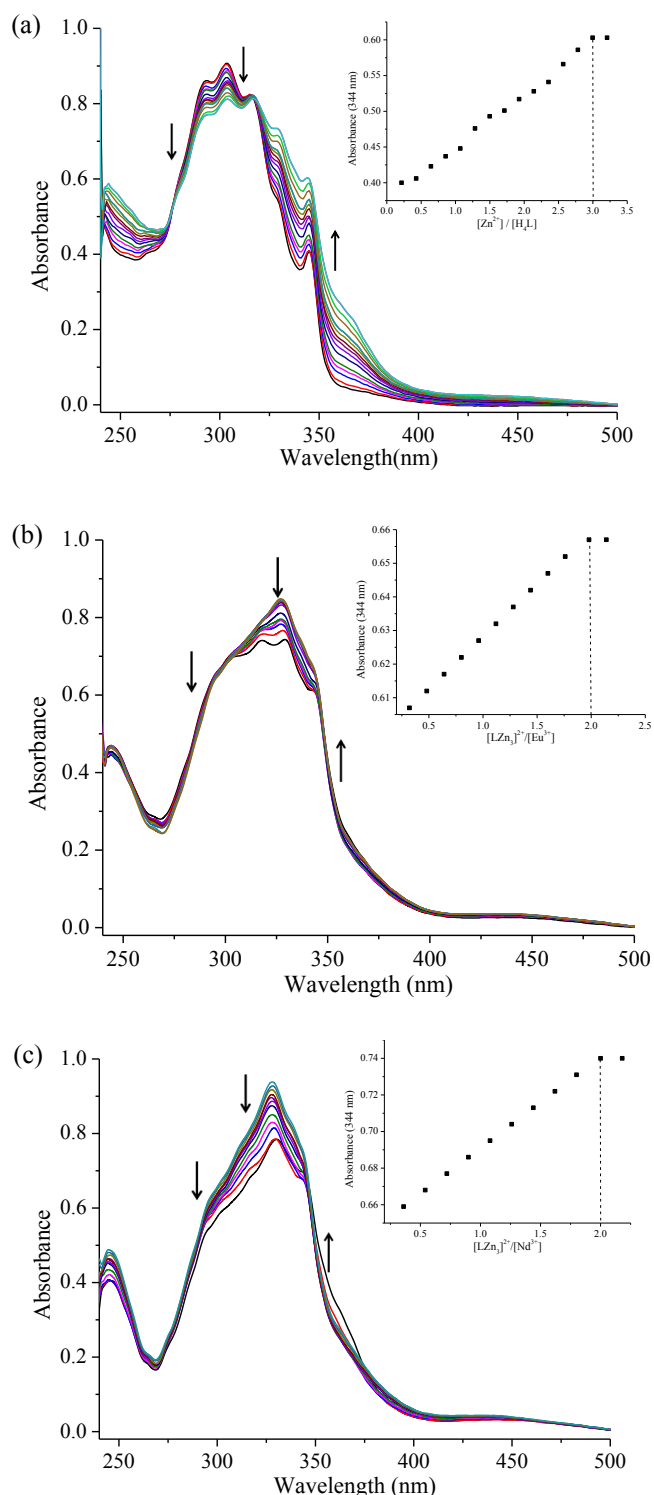


Fig. 2. UV-Vis spectra of the changes in the H_4L upon addition of (a) $Zn(OAc)_2$; (b) $Eu(NO_3)_3$; (c) $Nd(NO_3)_3$.

Yield, 38.2%. *Anal. Calc.* for $[Zn_4(L)_2Eu(NO_3)_3(H_2O)]$ ($C_{68}H_{54}Zn_4EuN_{11}O_{34}$): C, 41.19; H, 2.75; N, 7.77; Zn, 13.19; Eu, 7.66. Found: C, 41.30; H 2.88; N 7.64; Zn, 13.06; Eu, 7.51%. IR (KBr; cm^{-1}): 1607 [$\nu(C=N)$], 1254 [$\nu(Ar-O)$], 1741 [$\nu(C=O)$]. UV-Vis [in ethanol], λ_{max} (nm) [1.0×10^{-3} M]: 294, 313, 320, 361.

For $[Zn_4Nd]$ complex 3, block-like transparent light yellow crystals. Yield: 32.0%. Analytical calculation for $[Zn_4(L)_2Nd(NO_3)_3(H_2O)] \cdot CH_3CH_2OH$ ($C_{70}H_{60}Zn_4NdN_{11}O_{35}$): C, 41.60; H, 2.99; N,

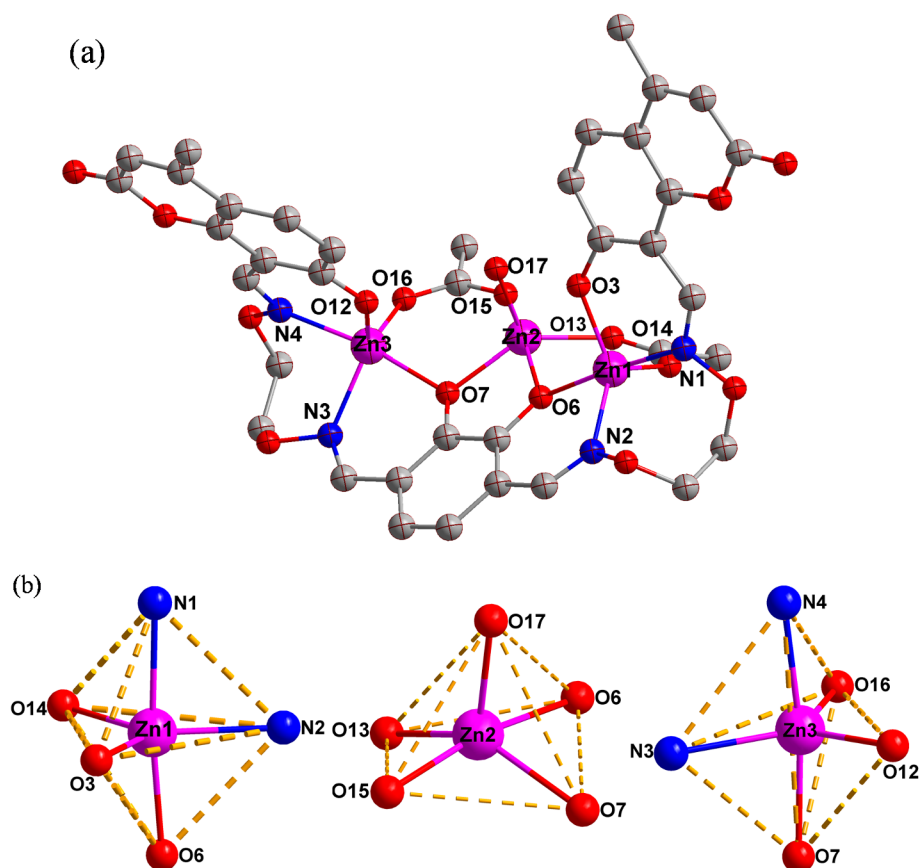


Fig. 3. (a) Molecular structure of complex 1; (b) Coordination polyhedra for Zn^{II} atoms of complex 1.

7.62; Zn, 12.94; Nd, 7.14. Found (%): C, 41.72; H, 3.07; N 7.53; Zn, 12.81; Nd, 7.02%. IR (KBr; cm^{-1}): 1605 [$\nu(C=N)$], 1240 [$\nu(Ar-O)$], 1730 [$\nu(C=O)$], 3415 [$\nu(O-H)$]. UV-Vis [in ethanol], λ_{max} (nm) [1.0×10^{-3} M]: 296, 315, 319, 358.

2.5. X-ray crystallographic analysis

Suitable single crystals of complexes 1–3 were mounted on glass rod for determining crystal structures. X-ray diffraction data of complexes 1–3 were performed on a SuperNova (Dual, Cu at zero, Eos) diffractometer using the graphite monochromated $Cu K\alpha$ ($\lambda = 1.54184 \text{ \AA}$) and Mo $K\alpha$ ($\lambda = 0.71073 \text{ \AA}$) radiation sources at 173.00(10), 294.21(11), 173.00(10) K, respectively. Multi-scan absorption corrections were applied. Crystal structures were solved using direct methods and refined anisotropically by the full-matrix least-squares techniques based on F^2 with SHELX-2014 program. Contributions to scattering due to these very large solvent accessible VOID(S) in structure were removed using the SQUEEZE routine of PLATON, the structures were then refined again using the data generated. The non-hydrogen atoms were refined anisotropically with displacement parameters. The positions for hydrogen atoms were fixed on geometrically idealized positions and refined via a riding model. Selected data of parameters and refinement of complexes 1–3 are summarized in Table 1.

3. Results and discussion

The H_4L and its corresponding complexes 1–3 were synthesized and characterized by FT-IR, UV-Vis absorption spectra, single-crystal X-ray crystallography, Hirshfeld surfaces analyses and luminescent spectra.

3.1. FT-IR spectra

Infrared spectra of H_4L and its complexes 1–3 showed various bands within the region $4000\text{--}400 \text{ cm}^{-1}$ (Fig. 1).

Infrared spectra of H_4L exhibited a strong band at 3444 cm^{-1} which is connected with the phenolic O–H stretching vibration band. However, these bands were disappeared in complexes 1 and 2, indicating that the phenolic O–H groups of H_4L are fully deprotonated. A new O–H stretching vibration band in complex 3 was observed at around 3415 cm^{-1} corresponding to crystallizing ethanol molecule [13]. The observed band in H_4L at 1617 cm^{-1} was assigned to a characteristic C=N vibration. Meantime, these characteristic C=N vibration bands of complexes 1–3 were found at 1604, 1607 and 1605 cm^{-1} , respectively [23]. Complexes 1–3 were shifted to lower frequencies by $10\text{--}13 \text{ cm}^{-1}$, demonstrating the coordination of the nitrogen atoms with Zn^{II} atoms. The expected Ar-O vibration band of H_4L was seen at $ca. 1279 \text{ cm}^{-1}$. Nevertheless, these bands in complexes 1–3 shifted to 1181, 1254 and 1240 cm^{-1} , respectively, moving to low frequencies [29]. In the IR spectrum of H_4L , the typical C=O vibration band emerged at 1751 cm^{-1} , and those of complexes 1–3 were detected at approximately 1731, 1741 and 1730 cm^{-1} , respectively. Most important of all, two new medium intensity bands for complexes 1–3 appeared at approximately 523, 530 and 520 cm^{-1} corresponding to Zn–N bond, and two characteristic bands at 454, 464 and 457 cm^{-1} were attributed to the formation of Zn–O bonds [42]. The facts mentioned above are in accordance with the results of crystal X-ray diffractions.

3.2. UV-Vis absorption spectra

The UV-Vis titration spectra of H_4L in chloroform:ethanol ($v:v = 1:1$) solution ($2.5 \times 10^{-5} \text{ mol L}^{-1}$) and its corresponding

Table 2
Hydrogen bonding and C–H \cdots π interactions (\AA , $^\circ$) of complexes 1–3.

D – H \cdots A	d(D – H)	d(H \cdots A)	d(D \cdots A)	\angle D – X \cdots A	Symmetry code
Complex 1					
O17–H17A \cdots O3	0.84	2.09	2.660(5)	124	–
C10–H10 \cdots O2	0.93	2.29	2.681(6)	105	–
C11–H11B \cdots O14	0.97	2.51	3.332(6)	143	–
C22–H22A \cdots O16	0.97	2.35	3.197(7)	145	–
C23–H23 \cdots O10	0.93	2.27	2.654(6)	104	–
C6–H6 \cdots O11	0.93	2.53	3.423(8)	161	–x, 1–y, 1–z
C13–H13 \cdots O12	0.93	2.56	3.480(5)	172	–x, 1–y, –z
C12–H12A \cdots Cg1		3.00	3.758(5)	136	–x, 1–y, 1–z
Complex 2					
C11–H11 \cdots O2	0.93	2.32	2.681(8)	102	
C11–H11 \cdots O3	0.93	2.54	2.938(8)	106	3/2 – x, y, 3/2 – z
C24–H24 \cdots O10	0.93	2.35	2.698(6)	102	
C24–H24 \cdots O8	0.93	2.53	2.940(6)	107	3/2 – x, y, 3/2 – z
C27–H27 \cdots O14	0.93	2.50	3.223(7)	135	3/2 – x, y, 3/2 – z
C13–H13A \cdots O13	0.97	2.49	3.017(10)	114	2 – x, 1–y, 1–z
C32–H32 \cdots O7	0.93	2.48	3.342(8)	155	1/2 + x, –y, 1/2 + z
Complex 3					
C2–H2 \cdots O26	0.93	2.43	3.142(7)	133	
C11–H11 \cdots O2	0.93	2.33	2.701(6)	103	
C22–H22A \cdots O31	0.97	2.52	3.443(9)	160	
C24–H24 \cdots O10	0.93	2.32	2.670(6)	102	
C45–H45 \cdots O8	0.93	2.49	2.854(7)	104	
C45–H45 \cdots O13	0.93	2.33	2.688(8)	102	
C47–H47A \cdots O25	0.97	2.50	3.419(7)	158	
C61–H61 \cdots O32	0.93	2.44	3.157(8)	134	
C21–H21 \cdots O32	0.93	2.57	3.457(9)	160	1 – x, 1 – y, 2 – z
C22–H22B \cdots O3	0.97	2.45	3.157(7)	130	1/2 – x, –1/2 + y, 3/2 – z
C46–H46B \cdots O27	0.97	2.50	3.163(8)	125	1 – x, 1 – y, 1 – z
C55–H55 \cdots O23	0.93	2.39	3.272(6)	158	–1/2 + x, 3/2 – y, –1/2 + z
C65–H65 \cdots O19	0.93	2.59	3.496(8)	164	1/2 + x, 3/2 – y, 1/2 + z
C34–H34A \cdots Cg2		2.73	3.639(7)	159	–1 + x, y, z

Symmetry codes: Cg1 for complex 1 are the centroids of atoms C24–C29; Cg2 for complex 3 are the centroids of atoms C35–C36–C37–C38–C42–C43.

complexes 1–3 in ethanol solution ($1.0 \times 10^{-3} \text{ mol L}^{-1}$) were collected with the range of 250–550 nm and are shown in Fig. 2.

Obviously, UV-Vis spectrum of H₄L possessed four absorption peaks at approximately 285, 302, 316 and 344 nm, respectively. The first peak at 285 nm is appointed to the π - π^* transition and the second and third peaks at 302 and 316 nm are assigned to π - π^* transition of the C=N bonds [33]. The fourth peak at 344 nm is assigned to the n- π^* transitions for carbonyl group. However, complex 1 exhibited four absorption peaks at about 292, 312, 318 and 356 nm, which were bathochromically shifted [46]. The phenomenon mentioned above manifests the coordination of the H₄L with the Zn^{II} atom.

In the titration experiment of complex 1, the ethanol solution of Zn(OAc)₂ were added gradually to solution of H₄L, and then the colour of above solution turned yellow. After Zn^{II} ions were added in excess of 3 equiv, the absorbance kept stable. Evidently, the titration curve showed the formation of a 1:3 trinuclear Zn^{II} complex and is shown in Fig. 2(a). As the UV-Vis absorption spectra of complexes 1–3 are similar change and could obtain the same conclusions. Clearly, the spectroscopic titration displayed the formation of 2:4:1 (H₄L:Zn^{II}:Ln^{III}) pentanuclear complexes 2 and 3 and presented in Fig. 2(b) and (c).

3.3. Crystal structure descriptions

3.3.1. Crystal structure of complex 1

Single crystal X-ray crystallography revealed complex 1 is a 1:3 ((L)⁴⁻:Zn^{II}) trinuclear structure. Complex 1 crystallizes in a triclinic system, space group of P-1 and is comprised of three Zn^{II} atoms, one completely deprotonated (L)⁴⁻ units, one coordinated water molecule, two μ_2 -acetate anions and one crystallizing dichloromethane molecule. The molecular structure of complex 1 is presented in Fig. 3. Selected bond lengths and angles of complexes 1–3 are listed in Table S1.

As depicted in Fig. 3, three Zn^{II} atoms are five-coordinated. Zn1 and

Zn3 atoms locate into N₂O₂ cores of the ligand and are bound by four donor atoms (Zn1–N1, 2.130(4) \AA ; Zn1–N2, 2.102(3) \AA ; Zn1–O3, 1.975(3) \AA ; Zn1–O6, 2.038(3) \AA and Zn3–N3, 2.111(3) \AA ; Zn3–N4, 2.119(4) \AA ; Zn3–O7, 2.039(3) \AA ; Zn3–O12, 1.980(3) \AA) from the symmetrical completely deprotonated (L)⁴⁻ units and one oxygen (Zn1–O14, 1.992(3) \AA and Zn3–O16, 1.970(3) \AA) atom from two μ -acetate anion. Therefore, the Zn1 and Zn3 atoms form the slightly distorted trigonal bipyramidal geometries, which being calculated by τ values are estimated to be $\tau_1 = 0.766$ and $\tau_2 = 0.768$, respectively. Meanwhile, central Zn2 atom is also surrounded by oxygen atoms: two phenolic oxygen (Zn2–O6, 2.087(3) \AA and Zn2–O7, 2.041(3) \AA) atoms arising from two fully deprotonated (L)⁴⁻ units, and two oxygen (Zn2–O13, 1.988(3) \AA and Zn2–O15, 2.004(4) \AA) atoms of two μ -acetate anions, and one oxygen (Zn2–O17, 2.010(4) \AA) atom of one coordinated water molecule. Consequently, the central Zn2 atom possesses a geometry of slightly distorted tetragonal pyramid which being calculated by τ value is estimated to be $\tau_3 = 0.491$. The Zn1 \cdots Zn2 and Zn2 \cdots Zn3 distance are 3.456(4) and 3.402(4) \AA , respectively (Table S1).

Supra-molecular interactions of complex 1 are built by extensive hydrogen bonding and C–H \cdots π interactions, which play a significant role in the crystal structure. Major hydrogen bonding data of complexes 1–3 are presented in Table 2. Five pairs of intra-molecular O17–H17A \cdots O3, C10–H10 \cdots O2, C11–H11B \cdots O14, C22–H22A \cdots O16 and C23–H23 \cdots O10 hydrogen bonding interactions are shown in Fig. 4(a) [54–57]. In addition, a 2D supra-molecular architecture is connected by one pair of C–H \cdots π (C12–H12A \cdots Cg1 (Cg1: C24–C25–C26–C27–C28–C29)) interaction (Fig. 4(b)). With the help of C–H \cdots π and hydrogen bonding interactions, an infinite 3D supra-molecular structure is built in Fig. 4(c).

3.3.2. Crystal structure of complex 2

X-ray crystallography indicated the crystal structure of complex 2,

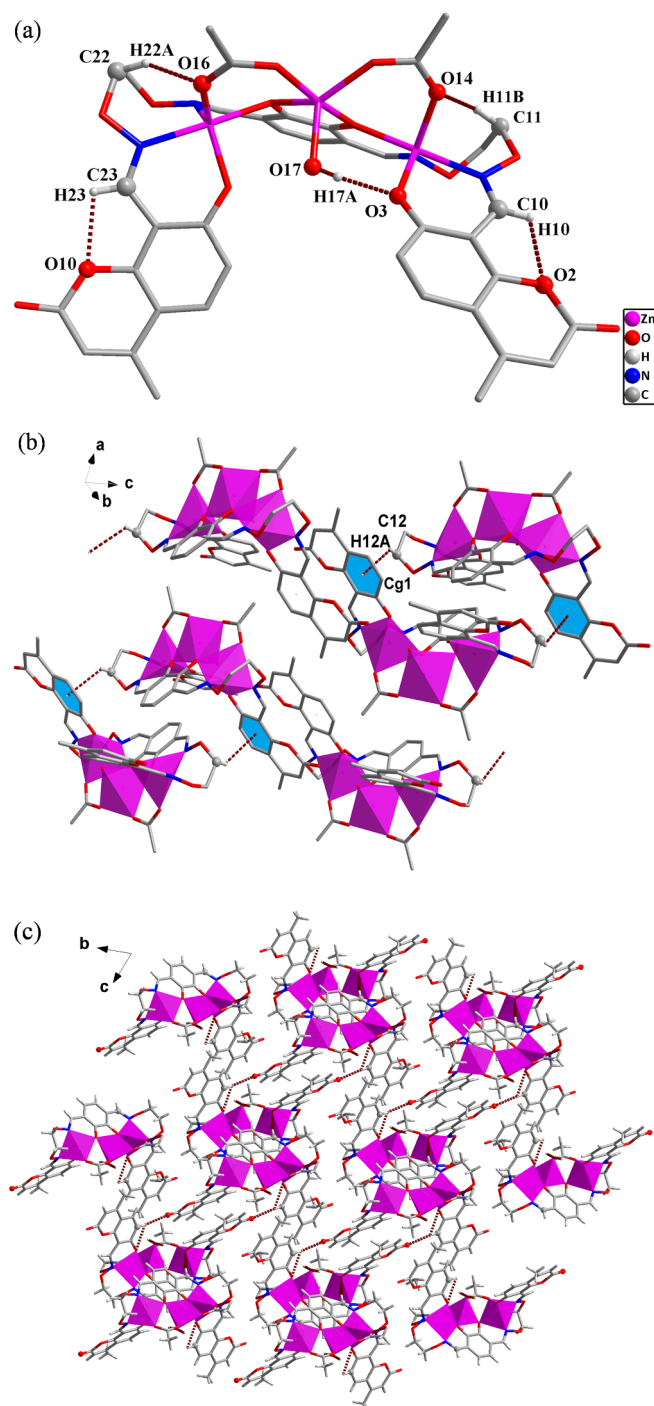


Fig. 4. (a) Intra-molecular hydrogen bonding interactions of complex 1; (b) C–H \cdots π interactions of complex 1; (c) 3D supra-molecular structure of complex 1.

which is different from complex 1 mentioned above. Complex 2 crystallizes in the monoclinic system, space group of $P2_1/n$, consisting of two fully deprotonated (L) $^{4-}$ units, four Zn^{II} atoms, one Eu^{III} atom, one coordinated water molecule and three coordinated NO_3^- anions. Therefore, complex 2 forms a rarely reported 2:4:1 ((L) $^{4-}$: Zn^{II} : Eu^{III}) hetero-pentannuclear structure [6] which is different from the previously reported structure of 1:1:1 [9,10,13,38], 1:2:1 [37] (L : M^{2+} : Ln^{3+}) of salamo-like complexes. The structure of complex 2 is illustrated in Fig. 5.

The Zn^{II} atoms ($Zn1$ and $Zn1^{#1}$) sited in N_2O_2 cores of the bis (salamo)-like ligands are embraced by four atoms ($N1$, $N2$, $O1AA$, $O5$ or

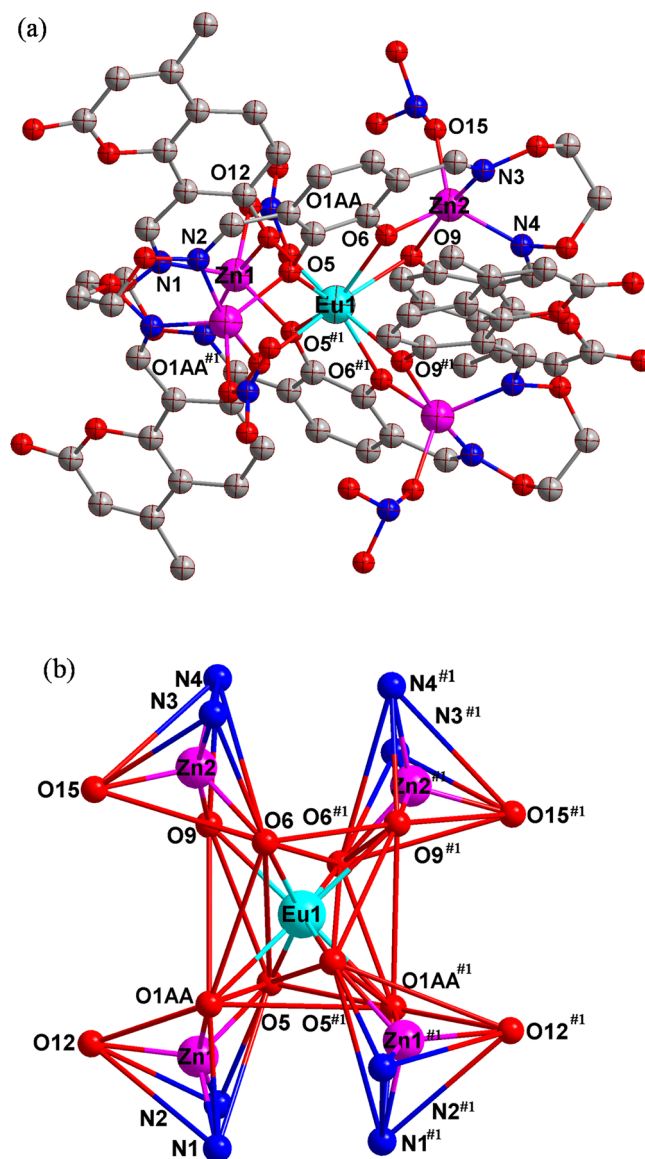


Fig. 5. (a) Molecular structure of complex 2; (b) Coordination polyhedra for Zn^{II} and Eu^{III} atoms of complex 2.

$N1^{#1}$, $N2^{#1}$, $O1AA^{#1}$) from the two fully deprotonated (L) $^{4-}$ units ($Zn1$ - $N1$, 2.044(4) Å; $Zn1$ - $N2$, 2.130(4) Å; $Zn1$ - $O1AA$, 2.095(3) Å and $Zn1$ - $O5$, 1.977(3) Å) and one oxygen ($Zn1$ - $O12$, 1.995(5) Å) atom of the coordinated NO_3^- anion. Therefore, the Zn^{II} atoms ($Zn1$ and $Zn1^{#1}$) are five-coordinated and form slightly distorted trigonal bipyramidal geometries with τ value is estimated to be $\tau_4 = 0.622$. Meantime, the other Zn^{II} atoms ($Zn2$ and $Zn2^{#1}$) are bonded by two nitrogen ($Zn2$ - $N3$, 2.130(4) Å and $Zn1$ - $N4$, 2.045(4) Å) atoms and two oxygen ($Zn2$ - $O6$, 1.978(3) Å and $Zn2$ - $O9$, 2.064(3) Å) atoms of two completely deprotonated (L) $^{4-}$ units, and one oxygen ($Zn2$ - $O15$, 1.985(4) Å) atom from half coordinated water and half coordinated NO_3^- molecule. Consequently, the Zn^{II} atom ($Zn2$ and $Zn2^{#1}$) is five-coordinated possessing the geometry of slightly distorted trigonal bipyramid with τ value is estimated to be $\tau_5 = 0.622$. The Eu^{III} atom is surrounded by eight phenolic oxygen ($Eu1$ - $O1AA$, 2.431(3) Å; $Eu1$ - $O5$, 2.420(3) Å; $Eu1$ - $O6$, 2.409(3) Å; $Eu1$ - $O9$, 2.449(3) Å; $Eu1$ - $O1AA^{#1}$, 2.431(3) Å; Eu - $O5^{#1}$, 2.420(3) Å; $Eu1$ - $O6^{#1}$, 2.409(3) Å and $Eu1$ - $O9^{#1}$, 2.449(3) Å) (Table S1) atoms from two fully deprotonated (L) $^{4-}$ ligands, and the Eu^{III} atom is eight-coordinated and possesses a distorted square antiprism geometry.

Moreover, five pairs of intra-molecular $C11$ - $H11$ \cdots $O2$, $C11$ -

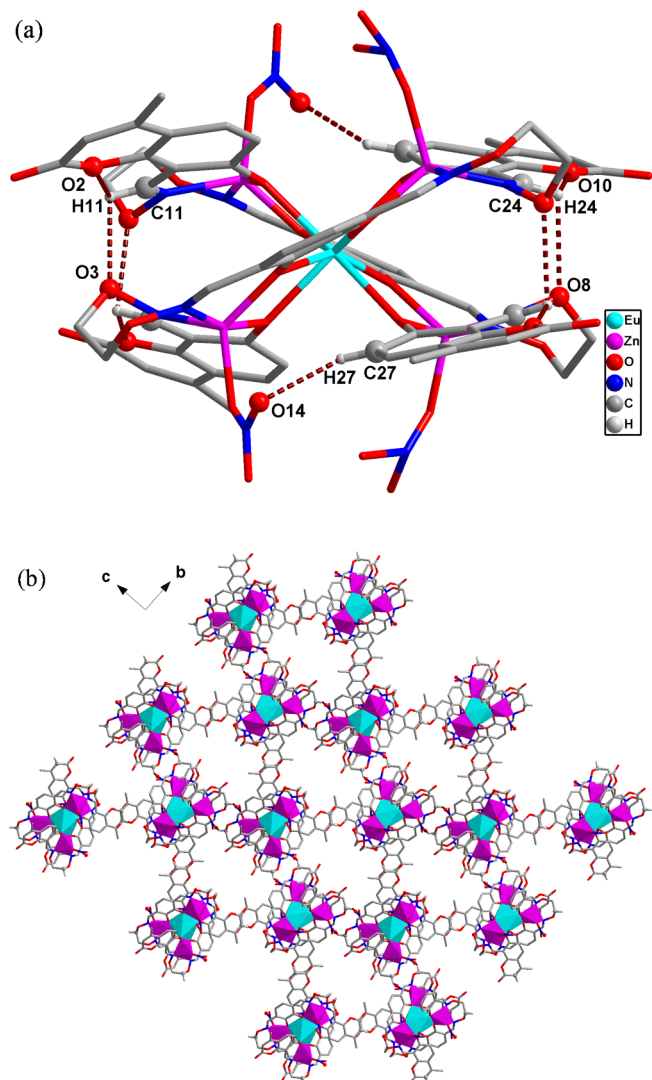


Fig. 6. (a) Intra-molecular hydrogen bonding interactions of complex 2; (b) 3D supra-molecular structure of complex 2.

H11 \cdots O3, C24-H24 \cdots O10, C24-H24 \cdots O8 and C27-H27 \cdots O14 hydrogen bonding interactions are shown in Fig. 6(a). An infinite 3D supra-molecular structure is linked by two pairs of intermolecular C13-H13A \cdots O13 and C32-H32 \cdots O7 hydrogen bonding interactions in Fig. 6(b) [58–60].

3.3.3. Crystal structure of complex 3

X-ray crystallography showed the crystal structure of complex 3 is a 2:4:1 ((L)⁴⁻:Zn^{II}:Nd^{III}) hetero-pentanuclear structure, which is similar to that of complex 2 mentioned above. Complex 3 crystallizes in the monoclinic system, space group of *P*2₁/*n* and is made up of four Zn^{II} atoms, one Nd^{III} atom, two fully deprotonated (L)⁴⁻ units, three coordinated NO₃⁻ anions, one coordinated water molecule and one crystallizing ethanol molecule. The crystal structure of complex 3 is shown in Fig. 7.

As shown in Fig. 7, all Zn^{II} atoms are located into N₂O₂ cavities from the two deprotonated (L)⁴⁻ units and five-coordinated with the same geometries. Zn1 atom is surrounded by two nitrogen (Zn1-N1, 2.034(4) Å and Zn1-N2, 2.111(4) Å) atoms and two oxygen (Zn1-O1, 2.067(3) Å and Zn1-O24, 1.968(3) Å) atoms from the fully deprotonated (L)⁴⁻ units, and one oxygen (Zn1-O35, 2.013(5) Å) atom from the coordinated water molecule. Therefore, Zn1 atom has a slightly distorted

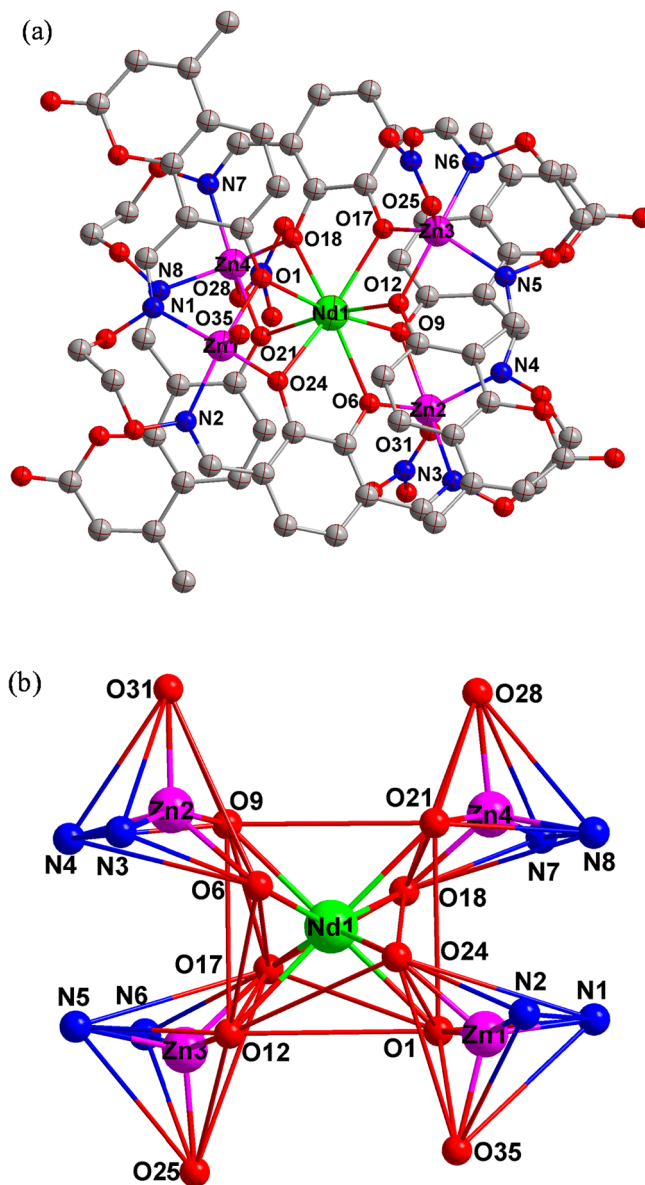


Fig. 7. (a) Molecular structure of complex 3; (b) Coordination polyhedra for Zn^{II} and Nd^{III} atoms of complex 3.

trigonal bipyramidal geometry, which being calculated by τ value is estimated to be $\tau_6 = 0.637$. Meanwhile, the other Zn^{II} atoms (Zn2, Zn3 and Zn4) are coordinated with several donor atoms (Zn2-N3, 2.133(5) Å; Zn2-N4, 2.043(4) Å; Zn2-O6, 1.969(4) Å; Zn2-O9, 2.105(3) Å; and Zn3-N5, 2.040(4) Å, Zn3-N6, 2.126(4) Å, Zn3-O12, 2.084(4) Å, Zn3-O17, 1.968(3) Å; and Zn4-N7, 2.115(4) Å, Zn4-N8, 2.034(4) Å, Zn4-O18, 1.959(3) Å, Zn4-O21, 2.083(3) Å) from the two (L)⁴⁻ units and three oxygen (Zn2-O31, 2.021(6) Å; Zn3-O25, 2.040(4) Å and Zn4-O28, 2.031(9) Å) atoms of the two coordinated NO₃⁻ anions (Table S1). Thus, the Zn2, Zn3 and Zn4 atoms have the slightly distorted trigonal bipyramidal geometries, which being calculated by τ values are estimated to be $\tau_7 = 0.518$, $\tau_8 = 0.606$ and $\tau_9 = 0.610$, respectively. Furthermore, the Nd^{III} atom is also embraced by eight phenolic oxygen atoms from the two bis(salamo)-like ligands. Thus, the Nd^{III} atom is eight-coordinated and possesses a distorted square antiprism geometry.

Supra-molecular interactants exist in complex 3. Eight pairs of intra-molecular C2-H2 \cdots O26, C11-H11 \cdots O2, C22-H22A \cdots O31, C24-H24 \cdots O10, C45-H45 \cdots O8, C45-H45 \cdots O13, C47-H47A \cdots O25 and C61-H61 \cdots O32 hydrogen bonding interactions are shown in Fig. 8(a)

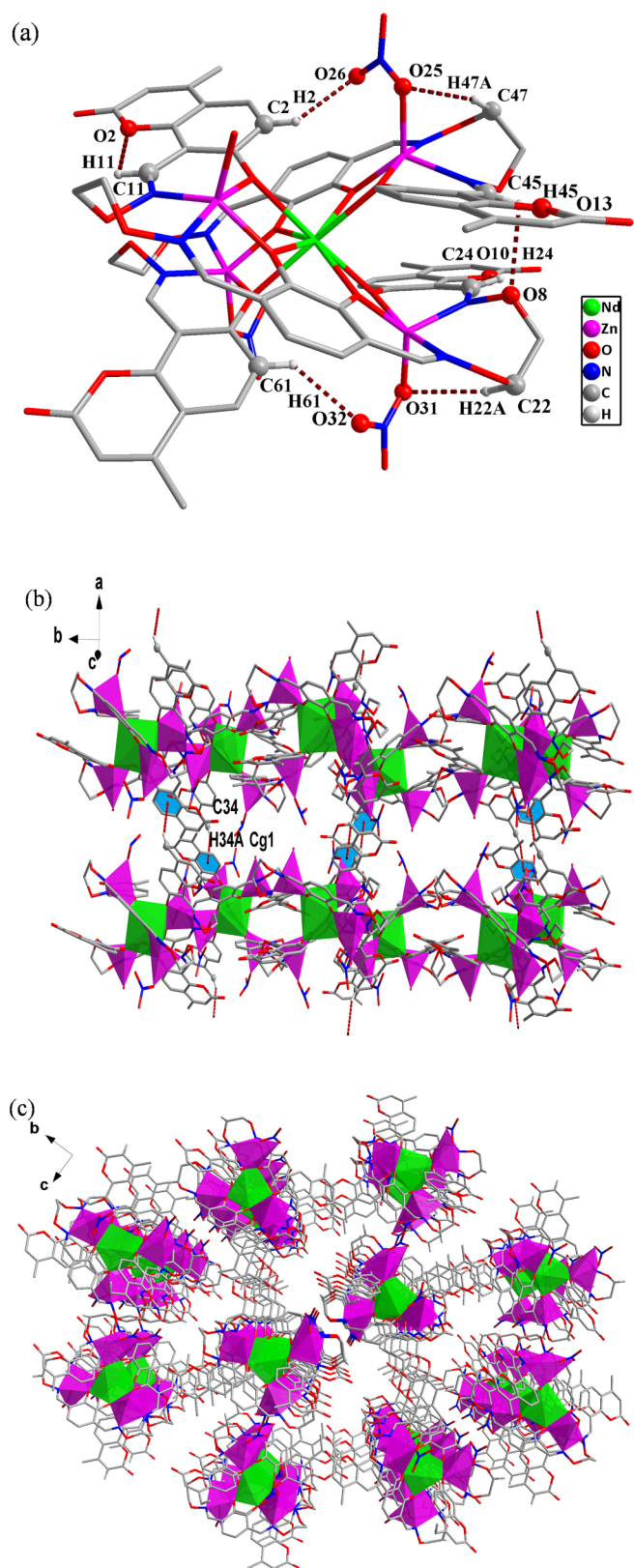


Fig. 8. (a) Intra-molecular hydrogen bonding interactions of complex 3; (b) C–H \cdots π interactions of complex 3; (c) 3D supra-molecular structure of complex 3.

[61,62]. In addition, a 2D supra-molecular architecture is built by C–H \cdots π (C34–H34A \cdots Cg2 (Cg2: C35–C36–C37–C38–C42–C43)) interactions in Fig. 8(b) [63,64]. A complicated 3D supra-molecular structure is observed in Fig. 8(c).

3.4. Hirshfeld surfaces analyses

The Hirshfeld surface analyses and 2D fingerprint plots of complex 1 were carried out using Crystal Explorer program. Complexes 2 and 3 did not undergo Hirshfeld surfaces analyses due to the presence of rare earth ions. For each point on the Hirshfeld isosurface, two distances, d_e (the distance from the point to the nearest nucleus external to the surface) and d_i (the distance to the nearest nucleus internal to the surface), are defined. They have been mapped with d_{norm} (standard high resolution), d_e , d_i , shape index and curvedness, and are illustrated in Fig. 9 [65].

When mapped with the d_{norm} , the surface of H₄L produces spherical red depressions, indicating the presence of mainly of the type C–H \cdots O interactions and other visible depressions correspond to H \cdots H and C \cdots H interactions. More intense red depressions in complex 1 are seen on the Hirshfeld surfaces which marks the O \cdots H/H \cdots O interactions persisting. The 2D fingerprint plots could explain the atom pair contacts of complex 1, which could quantify the intermolecular interactions. Meanwhile, it could be decomposed to highlight contributions from different interactions. The 2D fingerprint plots of C \cdots H/H \cdots C, H \cdots H and O \cdots H/H \cdots O interactions of complex 1 are depicted in Fig. 10. The proportion of C \cdots H/H \cdots C, interaction in complex 1 covers 8.4% of the Hirshfeld surfaces, and the proportions of H \cdots H and O \cdots H/H \cdots O interactions in complex 1 and cover 35.9 and 13.9%, respectively. As can be seen from the above facts, the proportions of H \cdots H is relatively stronger than C \cdots H/H \cdots C and O \cdots H/H \cdots O interactions [66].

3.5. Luminescences

In view of the excellent luminescent properties of zinc(II) and coumarin, the luminescent behaviors of H₄L and its corresponding complexes 1–3 were measured in ethanol solution (1.0×10^{-3} M) within wavelength range of 330–650 nm and displayed in Fig. 11. According to the spectra, H₄L upon excitation at 315 nm exhibited a strong emission peak at 386 nm and that could be attributed to intra-ligand π – π^* transitions [67,68]. Furthermore, the spectrum of complexes 1–3 displayed relatively weak emission peaks at ca. 515, 508 and 513 nm upon excitation at 315 nm, respectively. Compared to H₄L, three emission peaks of complexes 1–3 are bathochromically-shifted and that could be assigned to L–M charge-transfer transitions (LMCT) due to the coordination of nitrogen and oxygen atoms to metal (Zn^{II}, Eu^{III} and Nd^{III}) atoms [13,36].

4. Conclusions

Three homo-trinuclear Zn^{II} and hetero-pentanuclear Zn^{II}–Ln^{III} (Ln = Eu, Nd) complexes with a containing coumarin-skeleton bis (salamo)-like ligand H₄L were synthesized and structurally characterized. In complexes 1–3, all Zn^{II} atoms are located in the N₂O₂ sites and Eu/Nd^{III} atoms are embraced by eight phenolic oxygen atoms from the two fully deprotonated (L)⁴⁻ units. All the complexes have abundant hydrogen bonding and C–H \cdots π interactions. The Hirshfeld surfaces and 2D fingerprint plots can explain the atom pair contacts of the crystal, which can quantify the intermolecular interactions. Compared to H₄L, the luminescences of complexes 1–3 show bathochromically-shifted

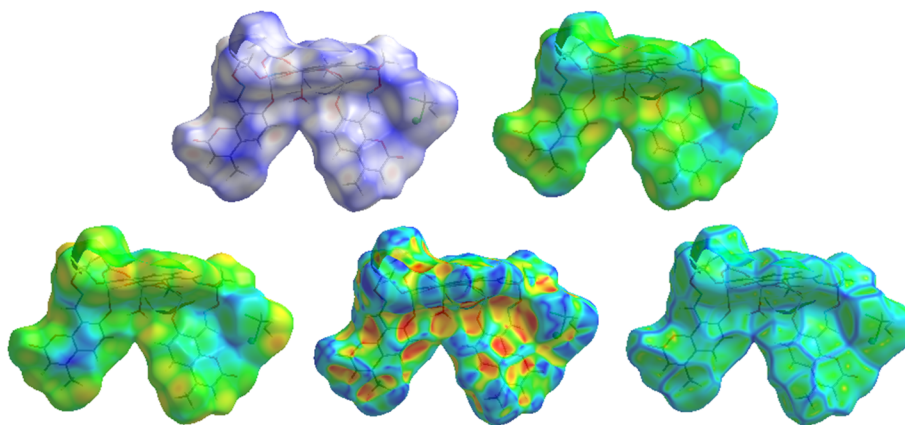


Fig. 9. Hirshfeld surfaces of complex 1 mapped with d_{norm} , d_e , d_i , shape index and curvedness.

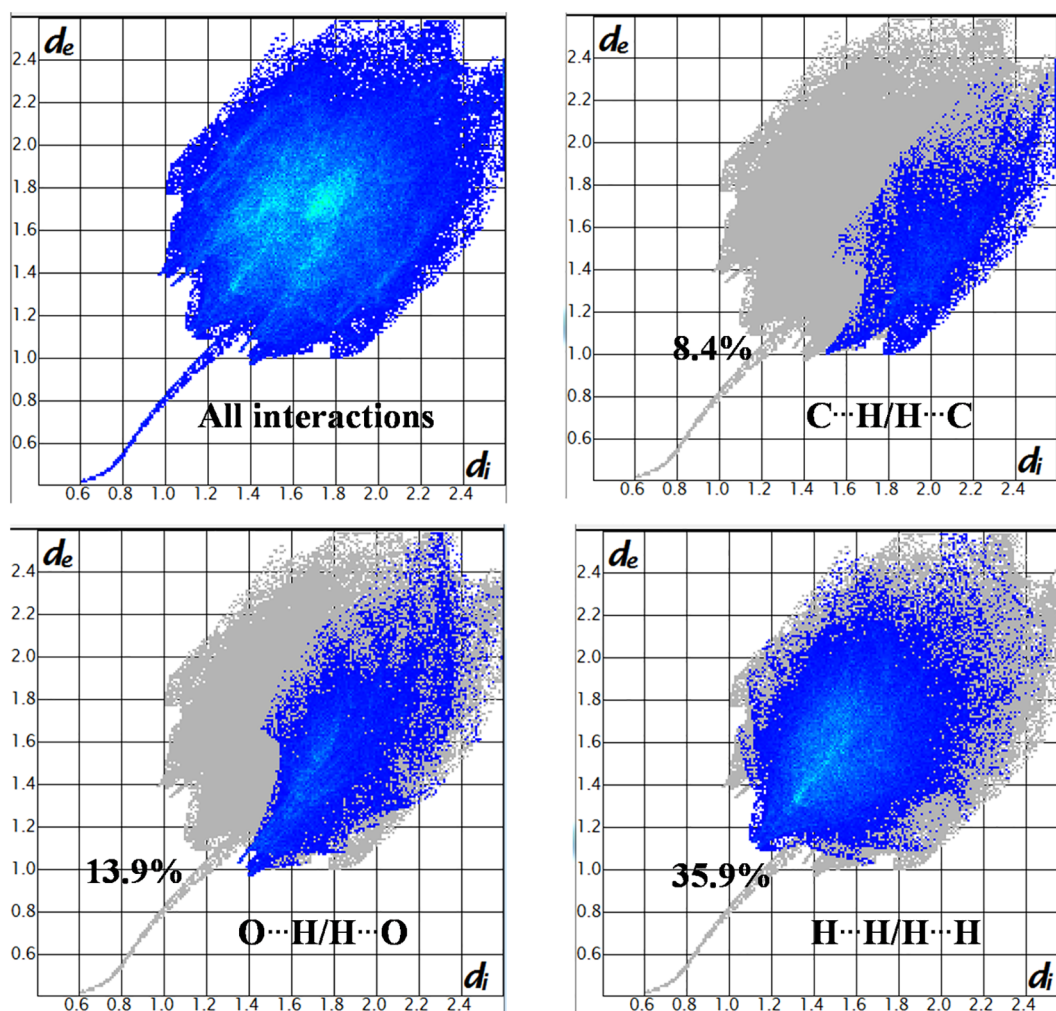


Fig. 10. 2D fingerprint plots of complex 1 with the major decomposition plots.

owing to the coordination of nitrogen and oxygen atoms from H_4L with metal atoms, which can be further investigated as a new type of luminescent material.

Acknowledgements

This work was supported by the National Natural Science Foundation of China (21761018) and the Program for Excellent Team of Scientific Research in Lanzhou Jiaotong University (201706), which is gratefully acknowledged.

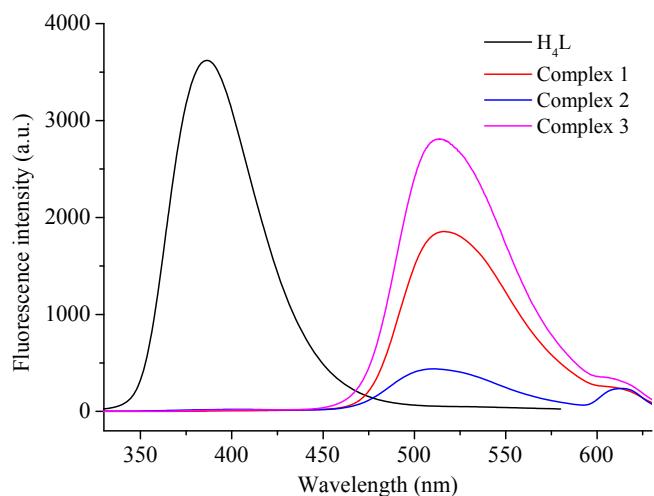


Fig. 11. Luminescences of H₄L and its complexes 1–3.

Appendix A. Supplementary data

CCDC 1888874, 1888872 and 1888873 contain the supplementary crystallographic data for complexes 1, 2 and 3. These data can be obtained free of charge via <http://www.ccdc.cam.ac.uk/conts/retrieving.html>, or from the Cambridge Crystallographic Data Centre, 12 Union Road, Cambridge CB2 1EZ, UK; fax: (+44) 1223-336-033; or e-mail: deposit@ccdc.cam.ac.uk. Supplementary data to this article can be found online at <https://doi.org/10.1016/j.ica.2019.02.040>.

References

- P.P. Liu, C.Y. Wang, M. Zhang, X.Q. Song, *Polyhedron* 129 (2017) 133.
- S. Akine, M. Miyashita, S. Piao, T. Nabeshima, *Inorg. Chem. Front.* 1 (2014) 53.
- X.Y. Li, L. Chen, L. Gao, Y. Zhang, S.F. Akogun, W.K. Dong, *RSC Adv.* 7 (2017) 35905.
- L.H. Li, W.K. Dong, Y. Zhang, S.F. Akogun, L. Xu, *Appl. Organometal Chem.* 31 (2017) e3818.
- T.K. Chin, S. Endud, S. Jamil, S. Budagumpi, H.O. Lintang, *Catal. Lett.* 143 (2013) 282.
- J. Hao, X.Y. Li, L. Wang, Y. Zhang, W.K. Dong, *Spectrochim. Acta Part A* 204 (2018) 388.
- L. Wang, J. Hao, L.X. Zhai, Y. Zhang, W.K. Dong, *Crystals* 7 (2017) 277.
- J. Li, H.J. Zhang, J. Chang, H.R. Jia, Y.X. Sun, Y.Q. Huang, *Crystals* 8 (2018) 176.
- W.K. Dong, J.C. Ma, Y.J. Dong, L.C. Zhu, Y. Zhang, *Polyhedron* 115 (2016) 228.
- W.K. Dong, J.C. Ma, L.C. Zhu, Y. Zhang, *New J. Chem.* 40 (2016) 6998.
- Y.A. Liu, C.Y. Wang, M. Zhang, X.Q. Song, *Polyhedron* 127 (2017) 278.
- X.Q. Song, P.P. Liu, Y.A. Liu, J.J. Zhou, X.L. Wang, *Dalton Trans.* 45 (2016) 8154.
- S.S. Zheng, W.K. Dong, Y. Zhang, L. Chen, Y.J. Dong, *New J. Chem.* 41 (2017) 4966.
- X.Y. Dong, S.F. Akogun, W.M. Zhou, W.K. Dong, *J. Chin. Chem. Soc.* 64 (2017) 412.
- Y.J. Dong, X.Y. Dong, W.K. Dong, Y. Zhang, L.S. Zhang, *Polyhedron* 123 (2017) 305.
- C.H. Tao, J.C. Ma, L.C. Zhu, Y. Zhang, W.K. Dong, *Polyhedron* 128 (2017) 38.
- W.K. Dong, J.C. Ma, Y.J. Dong, L. Zhao, L.C. Zhu, Y.X. Sun, Y.J. Zhang, *Coord. Chem.* 69 (2016) 3231.
- W.K. Dong, X.L. Li, L. Wang, Y. Zhang, Y.J. Ding, *Sens. Actuators B Chem.* 229 (2016) 370.
- B.J. Wang, W.K. Dong, Y. Zhang, S.F. Akogun, *Sens. Actuators B Chem.* 247 (2017) 254.
- F. Wang, L. Gao, Q. Zhao, Y. Zhang, W.K. Dong, Y.J. Ding, *Spectrochim. Acta Part A* 190 (2018) 111.
- B. Yu, C.Y. Li, Y.X. Sun, H.R. Jia, J.Q. Guo, J. Li, *Spectrochim. Acta Part A* 184 (2017) 249.
- J. Hao, X.Y. Li, Y. Zhang, W.K. Dong, *Materials* 11 (2018) 523.
- X.Y. Dong, X.Y. Li, L.Z. Liu, H. Zhang, Y.J. Ding, W.K. Dong, *RSC Adv.* 7 (2017) 48394.
- W.K. Dong, S.F. Akogun, Y. Zhang, Y.X. Sun, X.Y. Dong, *Sens. Actuators B Chem.* 238 (2017) 723.
- S. Di Bella, I. Fragala, *Synth. Met.* 115 (2000) 191.
- H.L. Wu, G.L. Pan, Y.C. Bai, H. Wang, J. Kong, F.R. Shi, Y.H. Zhang, X.L. Wang, *Res. Chem. Intermed.* 41 (2015) 3375.
- F. Wang, Y.L. Xu, S.O. Aderinto, H.P. Peng, H. Zhang, H.L. Wu, *J. Photochem. Photobiol. A* 332 (2017) 273.
- H.L. Wu, H. Wang, X.L. Wang, G.L. Pan, F.R. Shi, Y.H. Zhang, Y.C. Bai, J. Kong, *New J. Chem.* 38 (2014) 1052.
- L. Wang, X.Y. Li, Q. Zhao, L.H. Li, W.K. Dong, *RSC Adv.* 7 (2017) 48730.
- X.Y. Li, C. Liu, L. Gao, Y.X. Sun, Y. Zhang, W.K. Dong, *Polyhedron* 155 (2018) 320.
- J. Hao, L.H. Li, J.T. Zhang, S.F. Akogun, L. Wang, W.K. Dong, *Polyhedron* 134 (2017) 1.
- L. Chen, W.K. Dong, H. Zhang, Y. Zhang, Y.X. Sun, *Cryst. Growth Des.* 17 (2017) 3636.
- L. Gao, F. Wang, Q. Zhao, Y. Zhang, W.K. Dong, *Polyhedron* 139 (2018) 7.
- S. Akine, T. Taniguchi, T. Nabeshima, *Chem. Lett.* 30 (2001) 682.
- S. Akine, T. Taniguchi, T. Nabeshima, *Angew. Chem. Int. Ed.* 41 (2002) 4670.
- W.K. Dong, J.C. Ma, L.C. Zhu, Y. Zhang, *Cryst. Growth Des.* 16 (2016) 6903.
- X.Y. Dong, Q. Zhao, Q.P. Kang, H.R. Mu, H. Zhang, W.K. Dong, *Crystals* 8 (2018) 230.
- Y.C. Yang, Y. Zhang, Y. Meng, S.S. Zheng, W.K. Dong, *Chinese J. Inorg. Chem.* 34 (2018) 997.
- L.W. Zhang, L.Z. Liu, F. Wang, W.K. Dong, *Molecules* 23 (2018) 1141.
- Y.D. Peng, X.Y. Li, Q.P. Kang, G.X. An, Y. Zhang, W.K. Dong, *Crystals* 8 (2018) 107.
- Y.D. Peng, F. Wang, L. Gao, W.K. Dong, *J. Chin. Chem. Soc.* 65 (2018) 893.
- X.Y. Dong, Q.P. Kang, X.Y. Li, J.C. Ma, W.K. Dong, *Crystals* 8 (2018) 139.
- X.Q. Song, P.P. Liu, C.Y. Wang, Y.A. Liu, W.S. Liu, M. Zhang, *RSC Adv.* 7 (2017) 22692.
- H. Zhang, W.K. Dong, Y. Zhang, S.F. Akogun, *Polyhedron* 133 (2017) 279.
- L.W. Zhang, X.Y. Li, Q.P. Kang, L.Z. Liu, J.C. Ma, W.K. Dong, *Crystals* 8 (2018) 173.
- Q. Zhao, Z.L. Wei, Q.P. Kang, H. Zhang, W.K. Dong, *Spectrochim. Acta Part A* 203 (2018) 472.
- X.Y. Li, Q.P. Kang, L.Z. Liu, J.C. Ma, W.K. Dong, *Crystals* 8 (2018) 43.
- X.Y. Dong, Q. Zhao, Z.L. Wei, H.R. Mu, H. Zhang, W.K. Dong, *Molecules* 23 (2018) 1006.
- Q.P. Kang, X.Y. Li, Q. Zhao, J.C. Ma, W.K. Dong, *Appl. Organomet. Chem.* 32 (2018) e4379.
- X.Y. Dong, L. Gao, F. Wang, Y. Zhang, W.K. Dong, *Crystals* 7 (2017) 267.
- L. Gao, C. Liu, F. Wang, W.K. Dong, *Crystals* 8 (2018) 77.
- S. Akine, T. Taniguchi, T. Saiki, T. Nabeshima, *J. Am. Chem. Soc.* 127 (2005) 540.
- Y. Dong, J.F. Li, X.X. Jiang, F.Y. Song, Y.X. Cheng, C.J. Zhu, *Org. Lett.* 9 (2011) 2252.
- H.J. Zhang, J. Chang, H.R. Jia, Y.X. Sun, *Chinese J. Inorg. Chem.* 34 (2018) 2261.
- J. Chang, H.J. Zhang, H.R. Jia, Y.X. Sun, *Chinese J. Inorg. Chem.* 34 (2018) 2097.
- H.R. Jia, J. Chang, H.J. Zhang, J. Li, Y.X. Sun, *Crystals* 8 (2018) 272.
- Y.X. Sun, C.Y. Li, C.J. Yang, Y.Y. Zhao, J.Q. Guo, B. Yu, *Chinese J. Inorg. Chem.* 32 (2016) 327.
- Y.X. Sun, Y.Y. Zhao, C.Y. Li, B. Yu, J.Q. Guo, J. Li, *Chinese J. Inorg. Chem.* 32 (2016) 913.
- B. Yu, Y.X. Sun, C.J. Yang, J.Q. Guo, J. Li, Z. Anorg., *Allg. Chem.* 643 (2017) 689.
- J.Q. Guo, Y.X. Sun, B. Yu, J. Li, H.R. Jia, *Chinese J. Inorg. Chem.* 33 (2017) 1481.
- H.S. Zhang, K.Y. Zhang, L.C. Chen, Y.X. Li, L.Q. Chai, *J. Mol. Struct.* 1145 (2017) 32.
- L.Q. Chai, L. Zhou, K.Y. Zhang, H.S. Zhang, *Appl. Organometal. Chem.* 32 (2018) e4576.
- L. Zhou, Q. Hu, L.Q. Chai, K.H. Mao, H.S. Zhang, *Polyhedron* 158 (2019) 102.
- L.Q. Chai, Q. Hu, K.Y. Zhang, L. Zhou, J.J. Huang, *J. Lumin.* 203 (2018) 234.
- F. Wang, L.Z. Liu, L. Gao, W.K. Dong, *Spectrochim. Acta Part A* 203 (2018) 56.
- Y. Zhang, L.Z. Liu, Y.Q. Pan, W.K. Dong, *Crystals* 8 (2018) 259.
- L. Wang, Q.P. Kang, J. Hao, W.K. Dong, *Chin. J. Inorg. Chem.* 34 (2018) 525.
- H.R. Jia, J. Li, Y.X. Sun, J.Q. Guo, B. Yu, N. Wen, L. Xu, *Crystals* 7 (2017) 247.